

An enhancement mechanism of two-particle exchange interactions in single- and multi-layer cuprate superconductors

Shingo Teranishi*, Satoaki Miyao, Kazutaka Nishiguchi, and Koichi Kusakabe

Department of Materials Engineering Science, Graduate School of Engineering Science, Osaka University,
1-3 Machikaneyama-cho, Toyonaka Osaka 560-8531, Japan

To explore material dependence of layered cuprate superconductors, we examine effective two-particle interactions for Hg1201 and Tl1201, where Tl1201 having a nearly half value of T_c of Hg1201 even at the optimal oxygen concentration. Although the $3d_{x^2-y^2}$ band, the Fermi surface, and its Wannier-orbitals are similar for these superconductors, there is an apparent difference in the unoccupied levels above E_F . Based on a multi-reference density-functional-theory formulation, effective two-particle exchange interactions are estimated to derive enhancement in intra-layer exchange interactions for $\text{HgBa}_2\text{CuO}_4$, while it is weakened in TlBaLaCuO_5 and furthermore it is weak in $\text{TlBa}_2\text{CuO}_5$. The characteristic difference in the band structure is correlated with oxygen contents in the buffer layer. We also comment on the similar feature in triple-layered compounds. Our spin-fluctuation enhancement mechanism in an electron-correlation regime is consistent with the experimental fact.

1. Introduction

After the first discovery of a cuprate superconductor in 1986,¹⁾ plenty of cuprate superconductors have been reported.²⁻⁵⁾ Especially Hg-based cuprates are well known because of their high transition temperatures. For the high-temperature superconductivity (high T_c), in Hg-based cuprate crystal, the number n of CuO_2 planes should be three in a basic stacked-layered structure, *i.e.* in the unit cell. The critical temperature T_c for superconductivity rises up to 135K even at ambient pressure when a triple-layered Hg-based cuprate ($n = 3$) is chosen and when it is optimized with respect to its material parameters, *e.g.* the oxygen content.^{4,5)} Although several other compounds have similar superconducting properties, T_c becomes maximum by a choice of the material and by the adjustment of its internal material parameters.

To explore a basic mechanism of high- T_c , we reconsider several common features and detailed difference among cuprates, which should be explained by a unique theory. One of the special characters of high- T_c is material dependence of the superconducting properties. There are several known classification of cuprate superconductors in series, *e.g.* Hg-compounds, Tl-compounds, and Bi-compounds, which essentially differ in the atomic structure of the buffer layer. When we see some specific materials, and if we compare T_c of some compounds in different series, we can actually find several hints to understand the relevant superconducting mechanism.

We see global similarity in doping dependence of the CuO_2 planes. The optimal doping is often found at around a hole concentration of 0.16 per a CuO_2 plane. To adjust the concentration, one often needs to modify the buffer layers in its oxygen contents. When a high- T_c material is optimized with respect to the hole concentration, at the optimal doping, the layer-number dependence of the transition temperature T_c in several series of cuprates may be derived. Comparison among materials categorized in these series was made in experiment.⁶⁾ Triple-layer compounds provide the highest T_c among multi-layered compounds in various series. In addition, some special features of series dependence were con-

cluded, *e.g.* existence of a large n regime. When the layer number n becomes more than around 7, T_c reaches at a saturated value for each series. Actually, experimental findings of material dependence in nature always extend our understanding of the high- T_c superconductivity.

Theoretically, there are many successful explanations on tendency of the material dependence. An example was the Fermi surface shape dependence of several cuprate series.^{7,8)} In this direction, Sakakibara, *et al.* have explored that the single-layer Hg-based cuprate is in a good condition for the orbital distillation effect,⁹⁻¹¹⁾ while the 214 phase of La compounds may be a mixed multi- d -band system. They proposed that a purified $3d_{x^2-y^2}$ band for Hg-compounds should provides better high- T_c , while hybridization of $3d_{x^2-y^2}$ and $3d_{3z^2-r^2}$ components around the Fermi level may causes reduction in T_c . Even with this understanding, however, there remains unresolved material dependence.

Here an important hint can be found in the T_c difference between the Hg-series and the Tl-series. A known experimental fact is that T_c of Hg1201 is $T_c \approx 100\text{K}$ and that of Tl1201 is $T_c \approx 50\text{K}$ at the optimal doping.⁶⁾ Indeed, T_c of Tl1201 is only a half of the value of Hg1201. As we will show, the band structure calculation and the tight-binding fitting by the Wannierization technique^{12,13)} tell that relevant $3d_{x^2-y^2}$ bands of these compounds resemble each other. Conversely speaking, a single-band model derived by limited numbers of orbitals may not completely describe the material dependence.

On this problem, there had been several discussions on the T_c value and its dependence on materials parameters. The largeness of Madelung potential at the apical oxygen site,¹⁴⁾ the orbital energy difference between $3d_{x^2-y^2}$ and $3d_{3z^2-r^2}$ ⁹⁻¹¹⁾, the largeness of interlayer tunneling effect,¹⁵⁾ the lower amount of disorder on the CuO_2 plane were considered. As for the former three factors, however, the band structure calculation had captured the material characteristics as far as the single-particle transfer terms are concerned. The third effect should be reconsidered with careful consideration of two-particle parts relevant for the interlayer pair-hopping processes described by an effective Hamiltonian.¹⁶⁾ The last point

*teranishi@artemis.mp.es.osaka-u.ac.jp

would be experimental. However, we should note stiff nature of the cuprate high-temperature superconductivity against potential scatters.¹⁷⁾

Here, we propose another factor of the material dependence. We may discuss intra-layer effective exchange scattering between quasi-particles. The major contribution should be the super exchange mediated by the in-plane oxygen contributions. Actually, the famous Zhang-Rice mechanism of the singlet formation¹⁸⁾ taught us the relevance of the in-plane exchange interaction along each Cu-O-Cu bond for cuprates, which was described by a d - p model. There is, however, another exchange path mediated by elements even in the buffer layer. Owing to a renormalization formalism based on the multi-reference density functional theory (MR-DFT),¹⁹⁾ we can evaluate the material dependence of the exchange scattering among electrons in a CuO₂ plane. The formulation can start from any conventional DFT-based band structure calculation. By refining the representation from the single-reference to a multi-reference, an up-conversion Hamiltonian is defined. A relevant factor for our formulation is “the super process” inevitably concluded by the renormalized form of the strongly-correlated electron system.

In this paper, we analyze the band structures given by the generalized-gradient approximation of DFT. By comparing the energy bands of several Hg-based and Tl-based compounds, we deduce a factor deciding the super process, which may promote the strongly-correlated superconductivity. The Kohn-Sham orbitals as given by the band structure calculation may be used to make an expanding basis for a multi-reference representation of the strongly-correlated system. As a step forward to the full construction, we evaluate an exchange scattering path of two electrons around the hot-spots, which is mediated by the orbitals given by the buffer layers. As a result, we can find a material dependence in our enhancement mechanism of the spin-fluctuation mediated superconductivity.

2. Methods

2.1 Band structure calculation

In our MR-DFT formalism, we utilize an expression of an energy functional

$$\begin{aligned} & \bar{G}_{(C_i), \varepsilon_i}[\Psi] \\ &= \langle \Psi | \hat{T} + \hat{V}_{(C_i)} | \Psi \rangle + \frac{e^2}{2} \int d^3 r d^3 r' \frac{n_{\Psi}(\mathbf{r}) n_{\Psi}(\mathbf{r}')}{|\mathbf{r} - \mathbf{r}'|} \\ &+ E_{\varepsilon_i}[n_{\Psi}] + \int d^3 r v_{\text{ext}}(\mathbf{r}) n_{\Psi}(\mathbf{r}). \end{aligned} \quad (1)$$

Here $|\Psi\rangle$ is a state vector representing a multi-referenced correlated electron state and the charge density is given by $n_{\Psi}(\mathbf{r}) \equiv \langle \Psi | \hat{n}(\mathbf{r}) | \Psi \rangle$. An exchange-correlation energy-density functional $E_{\varepsilon_i}[n_{\Psi}]$ is given in an approximated form as a model, so that it is differentiable with respect to the density. A quantum fluctuation part representing an electron-correlation effect in an explicit expression is given in a next form.

$$\begin{aligned} & \langle \Psi | \hat{V}_{(C_i)} | \Psi \rangle \\ &= \langle \Psi | P_A \hat{V}_{\text{ee}} P_A | \Psi \rangle + \langle \Psi | P_A \hat{V}_{\text{ee}} P_B | \Psi \rangle + \langle \Psi | P_B \hat{V}_{\text{ee}} P_A | \Psi \rangle \\ &- \int d^3 r d^3 r' \frac{e^2 \langle \Psi | P_A \hat{n}(\mathbf{r}) P_A | \Psi \rangle \langle \Psi | P_A \hat{n}(\mathbf{r}') P_A | \Psi \rangle}{2|\mathbf{r} - \mathbf{r}'|} \end{aligned}$$

$$\begin{aligned} &= \langle \Psi | \hat{V}_{\text{ee}} | \Psi \rangle - \langle \Psi | P_B \hat{V}_{\text{ee}} P_B | \Psi \rangle \\ &- \int d^3 r d^3 r' \frac{e^2 \langle \Psi | P_A \hat{n}(\mathbf{r}) P_A | \Psi \rangle \langle \Psi | P_A \hat{n}(\mathbf{r}') P_A | \Psi \rangle}{2|\mathbf{r} - \mathbf{r}'|}, \end{aligned} \quad (2)$$

where projection operators P_A and $P_B \equiv \hat{1} - P_A$ project a phase space of representation state vectors $\{|\Psi_A\rangle\}$, which is called the A-space from now on, and its complementary space. The complementary is called the B-space.

For this setup, we have a direct product form of $|\Psi_A\rangle \equiv P_A |\Psi\rangle = |\Phi_A\rangle \otimes |\Phi_0\rangle$ for the representation state vector and $|\Psi\rangle = |\Psi_A\rangle + |\Psi_B\rangle$. The state $|\Phi_A\rangle$ is a multi-referenced state with a representation in a linear combination of multi-Slater determinants. Elements in the combination of $|\Phi_A\rangle$ are defined in a selected set of bands in the Bloch representation (or orbitals in the Wannier representation), which are specified by the orbital set A . In a usual correlated electron system, the complementary A^c of A is given by filled core levels, which may include semi-core states, and empty bands in high energy. The core state may be given as

$$|\Phi_0\rangle = \prod_{l \in A^c, \varepsilon_l \leq E_F} c_{l\uparrow}^\dagger c_{l\downarrow}^\dagger |0\rangle.$$

The definition of A and the resulted set $\{|\Psi_A\rangle\}$ may be given by a single-particle part of a total effective Hamiltonian given by

$$\mathcal{H}_{(C_i)} |\Psi\rangle = \frac{\delta \bar{G}_{(C_i), \varepsilon_i}[\Psi]}{\delta \langle \Psi |} \quad (3)$$

$$\mathcal{H}_{(C_i)} = \mathcal{H}_{(C_i)}^1 + \mathcal{H}_{(C_i)}^2 + \mathcal{H}_{(C_i)}^{1c}, \quad (4)$$

$$\mathcal{H}_{(C_i)}^1 = \hat{T} + \int \bar{v}_{\text{eff}, i}(\mathbf{r}) \hat{n}(\mathbf{r}) d^3 r, \quad (5)$$

$$\mathcal{H}_{(C_i)}^2 = P_A \hat{V}_{\text{ee}} P_A + P_A \hat{V}_{\text{ee}} P_B + P_B \hat{V}_{\text{ee}} P_A \quad (6)$$

$$\mathcal{H}_{(C_i)}^{1c} = - \int d^3 r d^3 r' \frac{e^2 \langle \Psi | P_A \hat{n}(\mathbf{r}') P_A | \Psi \rangle}{|\mathbf{r} - \mathbf{r}'|} P_A \hat{n}(\mathbf{r}) P_A. \quad (7)$$

Actually, the single-particle effective Hamiltonian $\mathcal{H}_{(C_i)}^1$ is given by an effective potential $\bar{v}_{\text{eff}}(\mathbf{r})$,

$$\bar{v}_{\text{eff}, i}(\mathbf{r}) = \int \frac{n(\mathbf{r}')}{|\mathbf{r} - \mathbf{r}'|} d^3 r' + \mu_{\varepsilon_i}(\mathbf{r}) + v_{\text{ext}}(\mathbf{r}), \quad (8)$$

and we have a counter part $\mathcal{H}_{(C_i)}^{1c}$ defined above. Here, contributions in $\bar{v}_{\text{eff}, i}(\mathbf{r})$ are the Hartree contribution, the model-exchange-correlation potential part,

$$\mu_{\varepsilon_i}(\mathbf{r}) = \frac{\delta E_{\varepsilon_i}[n]}{\delta n(\mathbf{r})}, \quad (9)$$

and the external potential $v_{\text{ext}}(\mathbf{r})$ for the system. $v_{\text{ext}}(\mathbf{r})$ may contain a scalar potential contribution of the core electrons when the ionic core description is enough accurate. This ionic potential may be replaced by a pseudo-potential. Replacement of a valence orbital by the corresponding pseudo wave function may be allowed, if the quantum fluctuation contribution, requiring evaluation of the Coulomb scattering processes, is properly evaluated by a technique of the non-empirical pseudo potential method.

By letting the number of states in A larger, by reducing the model exchange-correlation contribution, we may make models in a series. When $P_A \rightarrow \hat{1}$, and when $\lim_{i \rightarrow \infty} E_{\varepsilon_i}[n] = 0$,

the effective Hamiltonian approaches to the original Coulomb Hamiltonian for the electron system, and $|\Psi\rangle$ becomes the exact state of the electron system. Conversely, when the set of correlated orbital becomes an empty set, $A = \phi$, $|\Phi_A\rangle$ vanishes, P_A projects only a single-reference state $|\Psi_A\rangle = |\Phi_0\rangle$, and our representation becomes an ordinary Kohn-Sham single-reference representation of DFT, and the effective Hamiltonian becomes the Kohn-Sham Hamiltonian without explicit two-body terms.

As a convenient approximation, we may utilize a known exchange-correlation energy functional with additional correlation term $\hat{V}_{(C)_i}$ for a small number of relevant orbitals, where the electrons show strong correlation effects. The charge density, when it is converged in a self-consistent calculation, is mainly composed of the low-energy orbitals as $|\Phi_0\rangle$ and an averaged contribution from $|\Phi_A\rangle$. In such a case, the counter term contribution via $\mathcal{H}_{(C)_i}^{1c}$ does not have a big effect for the electron charge density. This means that a set of Kohn-Sham orbitals determined by $\mathcal{H}_{(C)_i}^1$ with a converged density may give a good expanding basis for the MR-DFT description. The convergence may be tested by having difference from the reference density and the density given by a multi-reference state vector $|\Psi_A\rangle$.

For cuprate, it is partially tested by having the optimized atomic structure by a single-reference calculation and comparing the result with the experiment. If the result shows good coincidence, inclusion of the low-energy correlation effect should not change the electron density so much from the approximated density. The correlation part $\hat{V}_{(C)_i}$ should only shift $|\Psi_A\rangle$ in a correlated state vector without big shift in the charge density. The momentum distribution function or the occupation of orbitals counted by $|\Psi_A\rangle$ become indicators for this test.

In this paper, for the derivation of the single-particle effective Hamiltonian, we adopt the Perdew-Burke-Ernzerhof formula of the generalized gradient approximation²⁰⁾ in DFT for the exchange correlation energy functional. This self-consistent scheme is known to be accurate enough to reproduce crystal parameters and to determine tight-binding parameters for various cuprates. Therefore, the inclusion of the effective two-body part should not change the global feature of effective occupation numbers of the Kohn-Sham orbitals and the charge density.

2.2 An effective up-conversion Hamiltonian

Even though the structural parameters are well reproduced by conventional methods of DFT, in order to describe the strong-correlation effects for the high- T_c materials, we need to incorporate the correlation effect into our effective model Hamiltonian. This is naturally done by including $\langle\Psi|\hat{V}_{(C)_i}|\Psi\rangle$ in our wave-function functional $\bar{G}_{(C)_i, \varepsilon_i}$. While the Kohn-Sham scheme is given by letting $\langle\Psi|\hat{V}_{(C)_i}|\Psi\rangle \equiv 0$. Therefore, we need to up-convert the ordinary Kohn-Sham Hamiltonian to a multi-referenced correlated model including $\langle\Psi|\hat{V}_{(C)_i}|\Psi\rangle$.

In our description, we have a set of correlated bands coming from the Cu $3d_{x^2-y^2}$ orbitals for cuprate. These bands are known to be well-defined in the DFT band structure. In this paper, we make a choice of a representation where only the $3d_{x^2-y^2}$ band is relevant for the set A , $|\Psi_A\rangle$, and the A-space. The selection of the set A for the $3d_{x^2-y^2}$ orbital may be done using the Wannierization transformation. However, since our

formalism is flexible, we may make use of the Bloch representation for the definition of the set A .

Once we have the A-space, the representation of $|\Psi\rangle = |\Psi_A\rangle + |\Psi_B\rangle$ allows us to rewrite the determination equation $\mathcal{H}_{(C)_i}|\Psi\rangle = E|\Psi\rangle$ into a simplified form. Since we fix the A-space representation, we omit the symbol $(C)_i$ to represent a specified model. In addition, we may rewrite the Hamiltonian into a form of $\mathcal{H} = \hat{H}_{AA} + \hat{h}_B + \hat{H}_{BA} + \hat{H}_{AB}$. Here, \hat{H}_{AA} is a many-body model Hamiltonian where each scattering of electrons happens only in orbitals of A . The operator \hat{h}_B is a single-particle Hamiltonian describing the orbital energy in A^c . Since we subtracted $\langle\Psi|P_B\hat{V}_{ee}P_B|\Psi\rangle$ in our definition of $\bar{G}_{(C)_i, \varepsilon_i}[\Psi]$, we have no direct interaction among particles in A^c orbitals. Namely, the quasi-particles in A^c are treated as non-interacting among them. The other two terms, \hat{H}_{BA} and \hat{H}_{AB} , represent interaction processes scattering at least one particle from an orbital in A to another in A^c or a reverse process. Please note that, owing to \hat{H}_{BA} and \hat{H}_{AB} , there appear indirect interactions among particles in A . Then, we can derive,

$$\begin{aligned} & (\hat{H}_A + \hat{h}_B)|\Psi_A\rangle \\ & + P_A\hat{H}_{AB}(E - \hat{H}_A - \hat{h}_B - P_B\hat{H}_{AB} - \hat{H}_{BA})^{-1}\hat{H}_{BA}P_A|\Psi_A\rangle \\ & = E|\Psi_A\rangle. \end{aligned} \quad (10)$$

This Brillouin-Wigner-type determination equation is exact. Here, the second term represents the super processes.

$$\hat{H}_{\text{super}} = P_A\hat{H}_{AB}(E - \hat{H}_A - \hat{h}_B - P_B\hat{H}_{AB} - \hat{H}_{BA})^{-1}\hat{H}_{BA}P_A. \quad (11)$$

This expression contains a resolvent operator, which actually generates many-particle Green functions in a real-frequency domain. This is because \hat{H}_{super} operates on a multi-reference state $|\Psi_A\rangle$ and its expectation value should be given only by a many-particle Green function.

If we note that the diagonal parts of \hat{H}_{AA} and \hat{h}_B do not change the number of electrons in the orbitals of A , and that \hat{H}_{BA} and \hat{H}_{AB} do change, we notice that the present form allows us to categorize the many-particle Green functions. Namely, when the resolvent in \hat{H}_{super} is counted, the Green function coming out of this expression should have a non-trivial quasi-particle number at least in one of an electron quasi particle set or a hole quasi particle set in A^c .

2.3 Two-particle scattering amplitudes

The last up-conversion Hamiltonian $\hat{H}_A + \hat{h}_B + \hat{H}_{\text{super}}$ defined by Eq. (10) is formally exact when we treat $\bar{G}_{(C)_i, \varepsilon_i}[\Psi]$ without approximation. The first term \hat{H}_A contains direct interactions among electrons in the correlated A orbitals. While, the super process \hat{H}_{super} represent indirect interactions for these correlated electrons. We can readily show that the screening effects owing to the electron-electron interaction are derived from \hat{H}_{super} . The screened effective interaction is given by summing the direct interaction of $P_A\hat{V}_{ee}P_A$ and \hat{H}_{super} . If we do a partial summation of the bubble diagrams appearing in \hat{H}_{super} , we may easily derive the RPA screening. The formally exact form of \hat{H}_{super} contains every scattering diagrams in the higher order. Actually, the ladder diagram can be readily derived from the expression of \hat{H}_{super} , and the vertex corrections are systematically derived.

In this paper, however, we focus on material dependence,

which may be well described by our \hat{H}_{super} . Therefore, we treat \hat{H}_{super} in an approximated manner. This expression contains final-state effects coming from the exact resolvent part. It requires a precise evaluation of high-energy steady states of the model system. However, for the analysis of cuprates, we may use a characteristic band structure, where the $3d_{x^2-y^2}$ band has a partial energy window. If the low-energy phenomena relevant for high- T_c happens essentially in a correlation effect within this energy range, we may treat material dependence of the effective low-energy scattering processes by utilizing a gap between the other bands. Namely, below the energy window around E_F of the DFT-GGA band, we have oxygen bands. Above the window, we have several high energy bands. Owing to the energy separation, we can safely evaluate a contribution from \hat{H}_{super} in an approximated manner by making a simple approximation for the resolvent.

In the exchange scattering, or the exchange interaction, it is well-known that the screening effect may not be relevant in general. In our evaluation of \hat{H}_{super} , due to the above-mentioned character of the band scheme, we may be allowed to evaluate the material dependence in the exchange scattering by neglecting the higher order screening effects. Actually, the screening of intra-band direct exchange process does not have relevant contribution compared to the indirect exchange process discussed in Sec. 3.2.

3. Results

3.1 Hg- and Tl-based cuprate compounds

For comparison, we consider Hg-compounds and Tl-compounds. When a cuprate crystal is prepared at an optimal doping, the structure often becomes an alloy or a mixed phase. To adopt a reliable DFT code²¹⁾ in our simulation, however, we need to consider a perfect periodic crystal with a unit cell. Therefore, the simulation becomes possible by limiting the filling factor at some special value allowing construction of a super cell. Owing to this reason, we treat a crystal phase fixing concentration of dopant and an oxygen composition ratio. In some cases, we look at a filling factor corresponding to the half-filling of the CuO_2 plane. Obtaining an expanding basis via DFT-GGA, our MR-DFT derives an effective many-body Hamiltonian, whose physical phase becomes a Mott insulating state for these cases. Note that the obtained band structure merely gives a spectrum of a single-particle part of the many-body effective Hamiltonian. For a good Mott insulator, therefore, the band structure of this single-particle part should show metallic features rather than an insulating gapped phase.

For the filling control, we mainly consider creation of oxygen deficiency. The oxygen concentration is controlled by reduction/oxidation of the buffer layers. Therefore, when we consider, for example, $\text{HgBa}_2\text{CuO}_{4+\delta}$ with δ from 0 to 1, we treat oxygen deficiency at the HgO_δ plane maintaining perfectness of CuO_2 layers. Similarly, when we consider three-layer $n = 3$ compounds, we consider the oxygen deficiency in the buffer layers. For the single-layer structures, we treat $\text{HgBa}_2\text{CuO}_4$ and $\text{TlBa}_2\text{CuO}_5$. The structural parameters for each crystal are determined by the optimization simulation in DFT-GGA, where the external pressure condition is zero. (Fig. 1)

$\text{HgBa}_2\text{CuO}_4$ lacks oxygen atoms at each HgO_δ plane. (Fig. 1 (a)) We have a local OHgO structure along the c axis. Oxygen atoms in this OHgO structure may be interpreted as

apical oxygen atoms of CuO_4 pyramids. While, $\text{TlBa}_2\text{CuO}_5$ has TlO planes. (Fig. 1 (b))

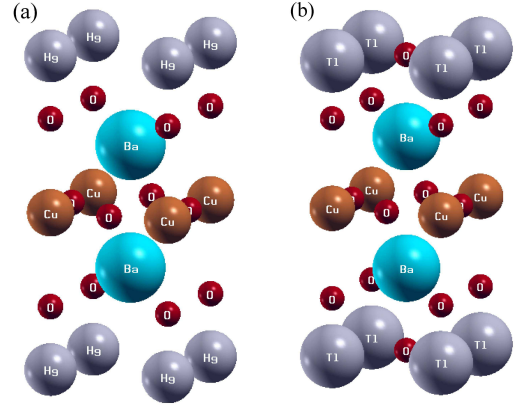


Fig. 1. The atomic structures of (a) $\text{HgBa}_2\text{CuO}_4$ (left) and (b) $\text{TlBa}_2\text{CuO}_5$ (right).

A nominal filling factor in the CuO_2 plane may be counted by the rule for ionization valence of noble metal, alkaline earth metal ions, and oxygen. Supposing Hg^{+2} , Tl^{+3} , Ba^{+2} , and O^{-2} , the Cu formal valence for these compounds are +2 (half-filling) for $\text{HgBa}_2\text{CuO}_4$ and +3 (one hole doped) for $\text{TlBa}_2\text{CuO}_5$. For Tl-compounds, we also examine TlBaLaCuO_5 in the discussion section, Sec. 4 where the Cu valence becomes +2 (half-filling).

As for the multi-layered cuprates, we focus on $n = 3$ in the following sections. Among the three layered compounds, we will consider Hg1223 and Tl1223 structures. Specifically, we treat $\text{HgBa}_2\text{Ca}_2\text{Cu}_3\text{O}_8$ and $\text{TlBa}_2\text{Ca}_2\text{Cu}_3\text{O}_9$. Their Cu valences are +2 (half-filling) and $+7/3$ ($1/3$ hole doping). Band structures of these compounds will be compared to derive a characteristic feature of the multi-layer compounds from our point of view.

3.2 Single-layer cuprate superconductors

We show the band structures of $\text{HgBa}_2\text{CuO}_4$, and $\text{TlBa}_2\text{CuO}_5$ in Fig. 2. In this calculation, we utilize the norm-conserving pseudo potentials with the PBE functional. The energy cut-offs in the plane-wave expansion for the wave function and the charge density are (100, 400) Ry. For the self-consistent charge density construction, the integration with respect to the k vectors is done using a $8 \times 8 \times 8$ k -point mesh in the 1st Brillouin zone. The unit cell of these compounds are optimized in the simulation, where the pressure control is done with a criterion of each diagonal element of the stress tensor being less than 0.5kbar. The internal atomic structures are optimized with a criterion that the summation of the absolute values of force vector elements becomes smaller than 1.0×10^{-8} [Ry/a.u.]. We adopted the wannierization method with the projection operators for the disentanglement process.^{12,13)}

The major parameters of the effective hopping Hamiltonian (the tight-binding model) for the $3d_{x^2-y^2}$ band of $\text{HgBa}_2\text{CuO}_4$ are similar to former estimations in the literatures.⁹⁾ In addition, the values of t , t' , and t'' are nearly the same for these

compounds. (Table I)

Table I. The parameters of the effective hopping hamiltonian for the $3d_{x^2-y^2}$ band in Hg1201, Tl1201 and Tl2201.

	Hg1201	Tl1201
t	-0.452	-0.574
t'	0.112	0.0990
t''	-0.100	-0.0823

Here, a little larger value of t for the Tl-compound comes from its shrunk lattice constant. When we use the lattice constant of Tl1201 for Hg1201, the value of t becomes close to -0.56. Considering change in T_c in high pressure for Hg-compound, the difference in the transition temperature can not be fully explained by the in-plane transfer parameters. Except when the effective screened interaction U is strongly material dependent, it is not easy to derive the reduction of T_c for Tl1201 by modeling with a single-band Hubbard Hamiltonian. We find that the oxygen bands coming from CuO_2 plane are also similar for these compounds. This is rather natural, because difference in the material structures among Hg1201 and Tl1201 compounds comes essentially from the buffer layers. The difference in the in-plane lattice constant is not enough large to modify the quantitative values of intra-layer hopping parameters.

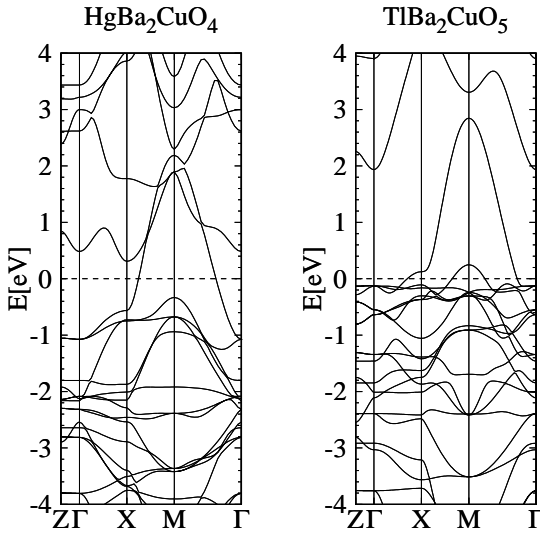


Fig. 2. Band structures of $\text{HgBa}_2\text{CuO}_4$ (left) and $\text{TlBa}_2\text{CuO}_5$ (right).

When we compare these band structures, an apparent difference is found in the low-lying unoccupied bands around E_F . For the $\text{HgBa}_2\text{CuO}_4$, it is the branch coming down to E_F around the X point and the Γ point. This band originates from the Hg 5p band. The partial density of states explicitly shows this character. The level is a hybridized orbital made from Hg 5p and apical oxygen 2p levels. Contrary to $\text{HgBa}_2\text{CuO}_4$, in the band structure of Tl1201, we have no signal of the low energy band at the X point. The Cu $3d_{x^2-y^2}$ band of $\text{TlBa}_2\text{CuO}_5$ is well isolated from the upper branches showing a good distillation in this sense. The speciality of $\text{TlBa}_2\text{CuO}_5$ becomes

further explicit by comparing this heavily hole-doped phase to La-doped Tl1201. In a crystal phase of TlBaLaCuO_5 , interestingly, we see the branch of TlO coming down to E_F around the Γ point.²²⁾ Therefore, this characteristic feature coming from the band structure has a good correlation with T_c of these compounds.

In our simulation method, we evaluated the exchange scattering amplitude of a process,

$$H_{\text{scat}} = \sum_{\mathbf{k}, \mathbf{k}', \sigma, \sigma'} J_{\mathbf{k}, \mathbf{k}'}^{\text{eff}} c_{\mathbf{k}', \sigma}^\dagger c_{\mathbf{k}, \sigma}^\dagger c_{\mathbf{k}', \sigma'} c_{\mathbf{k}, \sigma}. \quad (12)$$

Here, the amplitude is explicitly given by

$$J_{\mathbf{k}, \mathbf{k}'}^{\text{eff}} = - \sum_{\mathbf{K}, n \in A_1^c, m \in A_2^c} \frac{(V_{ee})_{\mathbf{k}, (m, \mathbf{K}) : (n, \mathbf{K}), \mathbf{k}} (V_{ee})_{(n, \mathbf{K}), \mathbf{k}' : \mathbf{k}' (m, \mathbf{K})}}{\varepsilon_{\mathbf{K}, n} + \tilde{\varepsilon}_{\mathbf{K}, m}}. \quad (13)$$

In the summation, $n \in A_1^c$ represents higher empty bands and $m \in A_2^c$ represents filled bands for holes. The amplitude of $(V_{ee})_{(n, \mathbf{K}), \mathbf{k}' : \mathbf{k}' (m, \mathbf{K})}$ is given by,

$$(V_{ee})_{(n, \mathbf{K}), \mathbf{k}' : \mathbf{k}' (m, \mathbf{K})} = \int d^3 r d^3 r' \frac{e^2 \phi_{\mathbf{k}'}^*(\mathbf{r}) \phi_{n, \mathbf{K}}^*(\mathbf{r}') \phi_{\mathbf{k}'}(\mathbf{r}') \phi_{m, \mathbf{K}}(\mathbf{r})}{2|\mathbf{r} - \mathbf{r}'|}. \quad (14)$$

Two types of Kohn-Sham orbitals are $\phi_{\mathbf{k}'}(\mathbf{r}')$ for the correlated $3d_{x^2-y^2}$ band and $\phi_{m, \mathbf{K}}(\mathbf{r})$ for the other levels in A^c . The process is schematically described by a Feynman diagram of Fig. 3. In the evaluation of J^{eff} , we used $4 \times 4 \times 4$ k-mesh points with the cut-off energy of (40, 160) Ry to save the computation time.

Since this process for *e.g.* a Hg compound is mediated by the Hg-band and the oxygen 2p band, it is not derived from a d - p model. Interestingly, the enhanced J^{eff} of O(10)meV is concluded for Hg1201 around the X point *i.e.* the hot spot. (Table II) However, for Tl1201, the value of J^{eff} is O(1)meV much smaller than the others, so that it would be negligible. When we adopt the spin-fluctuation mechanism in a correlated electron model, the enhanced exchange naturally have a positive effect to enhance T_c .

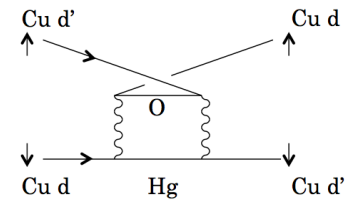


Fig. 3. Spin exchange process via low-lying quasi-particle (Hg) and quasi-hole (O) levels inducing enhanced electron correlation in Hg compounds.

Table II. Evaluated amplitudes for the exchange process in Hg1201, Tl1201 and La-doped Tl1201. The values $J_{X,Y}^{\text{eff}}$ are $J_{\mathbf{k}, \mathbf{k}'}^{\text{eff}}$ in eV when \mathbf{k} and \mathbf{k}' are at the X point and Y point, respectively.

	$\text{HgBa}_2\text{CuO}_4$	$\text{TlBa}_2\text{CuO}_5$	TlBaLaCuO_5
$J_{X,Y}^{\text{eff}}$	-0.04	0.004	-0.008

To show the relevance of the buffer layer structure, we mention a result for $\text{TlBa}_2\text{CuO}_4$. In this imaginative structure, we have the low-energy branch down even below E_F . Therefore, the reduction of oxygen contents in the buffer layer is rather important for this mechanism of enhancement in J^{eff} . Unfortunately, for the single-layer Tl compound, the mechanism seems not to be apparent for a reasonable value of oxygen contents for the superconductivity. This example rules the importance of oxygen atoms at the TlO layer, not only the apical oxygen and its geometrical parameter dependence.

Here we should note that $J_{\mathbf{k},\mathbf{k}'}^{\text{eff}}$ are in the momentum representation. There is no explicit z -component dependence on this value. So that the interaction is purely two dimensional. In the CuO_2 plane, the scattering coming from U has an amplitude U/N with the total number of mesh points in two-dimensional Brillouin zone. If we compare U/N with $N = 16$ to J^{eff} , we can say that the effect of the buffer layer to enhance the spin exchange is non negligible for some materials. There exists material dependent contribution for the enhancement as suggested by Table II.

If we consider a screening effect of the on-site Hubbard U , a larger reduction in the value of U should be expected when the higher (and lower) bands other than the correlated $3d_{x^2-y^2}$ band are take part in the screening process. Actually, our scheme suggests even lowered Hubbard U rather for $\text{HgBa}_2\text{CuO}_4$ than $\text{TlBa}_2\text{CuO}_5$. Therefore, the value of U may not be enough for the explanation of material dependence even if a modeling with the single band model is adopted. We expect that a relatively large U scheme with enhanced J^{eff} mediating the stronger spin fluctuation would be a solution for the explanation of known material dependence in T_c .

3.3 Triple-layer cuprate superconductors

In order to see that the mechanism derived for the single-layered cuprate in the last section may hold for the other multi-layer cuprates, we discuss the triple-layer phases of Hg- and Tl-compounds. In Fig. 4, we show the electronic band structure given by DFT-GGA simulations for $\text{HgBa}_2\text{Ca}_2\text{Cu}_3\text{O}_8$, $\text{TlBa}_2\text{Ca}_2\text{Cu}_3\text{O}_8$ and $\text{TlBa}_2\text{Ca}_2\text{Cu}_3\text{O}_9$.

In the Hg-based triple-layer compound, we see the Hg-O band coming down at the X point and the Γ point close to E_F . Therefore, the enhancement of J^{eff} is expected. Since the process is mediated by the Hg-O band, its effect should be bigger for the outer CuO_2 plan of this stacked CuO_2 layers. Experimentally, it is known that the superconductivity is much more stabilized for the outer plane than the inner plane. Our mechanism does not contradict to this known fact.

For the Tl-compounds, we use two typical crystal structures. The band structure of $\text{TlBa}_2\text{Ca}_2\text{Cu}_3\text{O}_9$ with 1/3 hole doping shows similar nature to $\text{TlBa}_2\text{CuO}_5$, where there are no higher branch close to E_F . We cannot expect the enhancement mechanism for this Tl compound. When we see an imaginative $\text{TlBa}_2\text{Ca}_2\text{Cu}_3\text{O}_8$, we see a branch of Tl-O coming down even below E_F . These two simulations suggest that the reduction in Tl-O layers may cause the Tl-O band downward. Suppose that the branch is just at a reasonable range when we adjust the oxygen content to make the optimal hole concentration,^{23,24)} our enhancement mechanism may contribute the high- T_c of the triple-layer phase of the Tl compound similar to Hg compounds. Therefore, as for our enhancement mechanism, it works nicely for Hg compounds when it is optimized

for the hole concentration. However, it may not work well when Tl compound is considered.

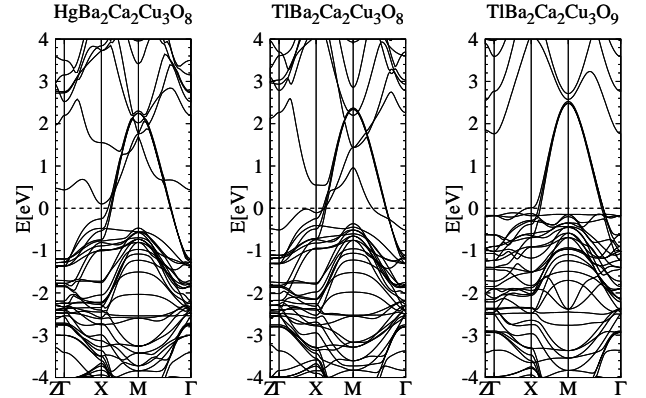


Fig. 4. Band structures of $\text{HgBa}_2\text{Ca}_2\text{Cu}_3\text{O}_8$ (left), $\text{TlBa}_2\text{Ca}_2\text{Cu}_3\text{O}_8$ (middle), and $\text{TlBa}_2\text{Ca}_2\text{Cu}_3\text{O}_9$ (right).

4. Discussion

In the last section, we derived material dependence among Hg- and Tl-compounds in the low-energy empty levels above E_F and the resulted enhancement in effective exchange scatterings. This mechanism to promote the spin-fluctuation mediated superconductivity is supported by the levels going down around the X point of the mercury compounds. One might suspect that the band effect may be originated by a special buffer layer with reduced amount of oxygen assumed for the simulation.

To assess the validity of our explanation for the real materials, we tested some material structures. One is $\text{HgBa}_2\text{CuO}_5$ to consider the real structure of hole-doped Hg1201. Since $\text{HgBa}_2\text{CuO}_5$ is an imaginative structure prepared for the test, the Cu valence becomes Cu^{+4} and the nominal hole concentration becomes two per Cu. The band structure shows no more low-lying branch at the X point. In that sense, our mechanism comes from the reduced buffer layers with small amount of oxygen. In the Hg compounds, however, the stoichiometry of $\text{HgBa}_2\text{CuO}_4$ corresponds to the half-filling. The global band structure is usually not so much affected by the inclusion of slight oxygen contents in the buffer layer. So, our mechanism and effective Hamiltonian derived using the end material should naturally work for the mercury compounds.

In Tl-compounds, it is not so easy to access the optimal doping by the reduction of the buffer layer. In a real Tl superconductor, La substitution was used to adjust the filling of CuO_2 . We tested TlBaLaCuO_5 , where the formal valence of Cu becomes +2. The result of the band structure calculation tells us that no signal of the low-energy branch at the X point. In the real material of $\text{TlBa}_{1-x}\text{La}_x\text{CuO}_5$, it is known that T_c does not reach the value over 50K even by adjusting the hole concentration.^{25,26)} Thus, we may propose to consider a careful control of oxygen in Tl1201 without La doping, which might make an enhancement of T_c . Actually, this way of approach is consistent with some reported facts.²⁷⁾

5. Summary and conclusions

In this paper, we introduced a simulation method of the exchange scattering amplitudes in cuprates based on our MR-DFT method. By applying the method, we evaluated an effective exchange scattering amplitude for some Hg and Tl compounds. Analyzing the nature of the electronic band structures of these compounds, we found that the high energy levels originated from the Hg-O buffer layer contributes well creating enhancement of J_{eff} , which should lead the increase in T_c via the spin fluctuation mechanism. In Tl compounds, however, the enhancement is not so apparent. This is because of the absence of the Tl-O branch around E_F . Our mechanism, which is consistent with the known experimental facts, may explain strange difference between T_c s of Hg- and Tl-compounds, thereby it may lead us to further approaches to create the new design of cuprate superconductors.

The calculations were done in the computer centers of Kyushu University and ISSP, University of Tokyo. The work is supported by joint-project for “Study of a simulation program for the correlated electron systems” with Advance-soft co. J161101009, and JSPS KAKENHI Grant Numbers JP26400357.

-
- 1) J. G. Bednorz and K. A. Müller: *Z. Physik B* **64** (1986) 267.
 - 2) M. K. Wu, J. R. Ashburn, C. J. Torng, P. H. Hor, R. L. Meng, L. Gao, Z. J. Huang, Y. Q. Wang, and C. W. Chu: *Phys. Rev. Lett.* **58** (1987) 908.
 - 3) S. Putilin, E. Antipov, O. Chmaissem, and M. Marezio: *Nature* **362** (1993) 226.
 - 4) A. Schilling, M. Cantoni, J. Guo, and H. Ott: *Nature* **363** (1993) 56.
 - 5) K. Isawa, A. Tokiwa-Yamamoto, M. Itoh, S. Adachi, and H. Yamauchi: *Physica C* **222** (1994) 33.
 - 6) H. Mukuda, S. Shimizu, A. Iyo, and Y. Kitaoka: *J. Phys. Soc. Jpn.* **81** (2012) 011008.
 - 7) E. Pavarini, I. Dasgupta, T. Saha-Dasgupta, O. Jepsen, and O. K. Andersen: *Phys. Rev. Lett.* **87** (2001) 047003.
 - 8) K. Tanaka, T. Yoshida, A. Fujimori, D. H. Lu, Z.-X. Shen, X.-J. Zhou, H. Eisaki, Z. Hussain, S. Uchida, Y. Aiura, K. Ono, T. Sugaya, T. Mizuno, and I. Terasaki: *Phys. Rev. B* **70** (2004) 092503.
 - 9) H. Sakakibara, H. Usui, K. Kuroki, R. Arita, and H. Aoki: *Phys. Rev. Lett.* **105** (2010) 2.
 - 10) H. Sakakibara, H. Usui, K. Kuroki, R. Arita, and H. Aoki: *Phys. Rev. B* **85** (2012) 1.
 - 11) H. Sakakibara, K. Suzuki, H. Usui, S. Miyao, I. Maruyama, K. Kusakabe, R. Arita, H. Aoki, and K. Kuroki: *Phys. Rev. B* **89** (2014) 6.
 - 12) N. Marzari and D. Vanderbilt: *Phys. Rev. B* **56** (1997) 12847.
 - 13) I. Souza, N. Marzari, and D. Vanderbilt: *Phys. Rev. B* **65** (2001) 035109.
 - 14) Y. Ohta, T. Tohyama, and S. Maekawa: *Phys. Rev. B* **43** (1991) 2968.
 - 15) P. Anderson: *Science* **268** (1995) 1154.
 - 16) K. Nishiguchi, K. Kuroki, R. Arita, T. Oka, and H. Aoki: *Phys. Rev. B* **88** (2013) 1.
 - 17) H. Eisaki, N. Kaneko, D. L. Feng, A. Damascelli, P. K. Mang, K. M. Shen, Z.-X. Shen, and M. Greven: *Phys. Rev. B* **69** (2004) 064512.
 - 18) F. C. Zhang and T. M. Rice: *Phys. Rev. B* **37** (1988) 3759.
 - 19) K. Kusakabe: *Journal of the Physical Society of Japan* **70** (2001) 2038.
 - 20) J. P. Perdew, K. Burke, and M. Ernzerhof: *Phys. Rev. Lett.* **77** (1996) 3865.
 - 21) P. Giannozzi, S. Baroni, N. Bonini, M. Calandra, R. Car, C. Cavazzoni, D. Ceresoli, G. L. Chiarotti, M. Cococcioni, I. Dabo, A. Dal Corso, S. de Gironcoli, S. Fabris, G. Fratesi, R. Gebauer, U. Gerstmann, C. Gougoussis, A. Kokalj, M. Lazzeri, L. Martin-Samos, N. Marzari, F. Mauri, R. Mazzarello, S. Paolini, A. Pasquarello, L. Paulatto, C. Sbraccia, S. Scandolo, G. Sclauzero, A. P. Seitsonen, A. Smogunov, P. Umari, and R. M. Wentzcovitch: *Journal of physics. Condensed matter : an Institute of Physics journal* **21** (2009) 395502.
 - 22) P. R. C. Kent, T. Saha-Dasgupta, O. Jepsen, O. K. Andersen, A. Macridin, T. A. Maier, M. Jarrell, and T. C. Schulthess: *Phys. Rev. B* **78** (2008) 035132.
 - 23) I. Hase, N. Hamada, A. Iyo, N. Terada, Y. Tanaka, and H. Ihara: *Physica C: Superconductivity* **357** (2001) 153.
 - 24) J. Liu, I. Chang, M. Lan, P. Klavins, and R. Shelton: *Physica C: Superconductivity* **246** (1995) 203.
 - 25) H. Ku, M. Tai, J. Shi, M. Shieh, S. Hsu, G. Hwang, D. Ling, T. Watson-Yang, and T. Lin: *Jpn. J. Appl. phys.* **28** (1989) L923.
 - 26) M. Subramanian, G. Kwei, J. Parise, J. Goldstone, and R. Von Dreele: *Physica C: Superconductivity* **166** (1990) 19.
 - 27) M. Subramanian: *Materials research bulletin* **29** (1994) 119.